

## Influence of Defective Formations on Photoconductivity of Layered Crystals with Cationic Substitution

A. Kashuba<sup>1,2,\*</sup>, B. Andriyevskyy<sup>3</sup>, I. Semkiv<sup>1</sup>, L. Andriyevska<sup>4</sup>, R. Petrus<sup>1</sup>, E. Zmiiovska<sup>1</sup>, D. Popovych<sup>5</sup>

<sup>1</sup> Lviv Polytechnic National University, Faculty of Physics, 12, S. Bandera Str., 79013 Lviv, Ukraine

<sup>2</sup> Ivan Franko National University of Lviv, Faculty of Electronics and Computer Technologies, 107, Tarnavsky Str., 79005 Lviv, Ukraine

<sup>3</sup> Faculty of Civil Engineering, Environmental and Geodetic Sciences, Koszalin University of Technology, 2, Śniadeckich Str., PL-75-453 Koszalin, Poland

<sup>4</sup> Faculty of Electronics and Computer Sciences, Koszalin University of Technology, 2, Śniadeckich Str., PL-75-453 Koszalin, Poland

<sup>5</sup> Pidstryhach Institute for Applied Problems of Mechanics and Mathematics NAS of Ukraine, 3-B, Naukova Str., Lviv, Ukraine

(Received 07 September 2018; revised manuscript received 07 December 2018; published online 18 December 2018)

The results of studying the electronic conductivity of  $\text{In}_x\text{Tl}_{1-x}\text{I}$  solid solutions of substitution are presented. The effective mass and mobility of an electron have been determined with using the first-principle calculations of the band-energy structure. The investigation was carried out for  $\text{In}_x\text{Tl}_{1-x}\text{I}$  solid solutions of substitution with the concentrations 0.125, 0.25, 0.375, 0.5, 0.625 of thallium. Dynamics of changes in the effective mass, mobility and conductivity as functions of the thallium content has been established. Peculiarities of the band-energy spectrum of defective structures (with anionic vacancies and cationic interstitials) have been investigated. Shapes of the conductivity spectrum and its transformation under the influence of defective formations have been studied.

**Keywords:** Semiconductors, Band structure, Effective mass, Mobility, Conductivity.

DOI: [10.21272/jnep.10\(6\).06025](https://doi.org/10.21272/jnep.10(6).06025)

PACS number: 72.20. – i

### 1. INTRODUCTION

For a long time, the attention of scientists is being focused on finding new materials with a controlled change in physical properties. In particular, these properties can be obtained by introducing impurities in already known crystals or by creating solid solutions based on them. Also, the stability of samples and easiness of their obtaining are an important condition.

Among recently synthesized new mixed semiconductors of the  $\text{A}^{\text{III}}\text{B}^{\text{V}}\text{VII}$  group there is three-component system  $\text{In}_x\text{Tl}_{1-x}\text{I}$  whose crystals represent a continuous series of solid solutions of substitution (SSS). Their band gap can vary within the range  $2.01 < E_g < 2.84$  eV [1-4]. These crystals possess a layered structure and in contrast with typical layered crystals of the  $\text{A}^{\text{II}}\text{B}^{\text{VI}}$  and  $\text{A}^{\text{III}}\text{B}^{\text{VI}}$  ( $\text{PbI}_2$ ,  $\text{CdI}_2$ ,  $\text{HgI}_2$ ,  $\text{GaSe}$ ,  $\text{InSe}$ ) groups [5], in which the Van der Waals gaps are formed anions, in these SSS  $\text{In}_x\text{Tl}_{1-x}\text{I}$  in the region of weak chemical bonding by nearest cations indium and thallium.

The combination of optical anisotropy and structural transformations in the  $\text{In}_x\text{Tl}_{1-x}\text{I}$  SSS makes the samples under study rather perspective for nonlinear optics and electrical engineering. In particular, in [1] the photoconductivity spectra were presented, where it was found that in the plane of the ac layer there is a current flow of *n*- and *p*-type. The authors suggest that the cause of the appearance of *n*-type conductivity is due to anionic vacancy, or cationic interstitials. This type of conductivity occurs in the crystallographic direction [1]. Since in this case, in the plane of an ac-layer, alternation of the quasimetal-dielectric chain

structures is possible, one can assume that the samples under study can be used as a material for low-dimensional capacitors. That is why the main purpose of this work is to determine what causes the *n*-type conductivity and quasimetallization of the connections in it.

Since, if at least one of the above assumptions [1] leads to a quasimetallization of the sample, this should not be reflected in the conductivity spectrum and band structure. The paper presents a study based on the first principles of conductivity for polarized and unpolarized light beams as well as the dynamics of change in the band spectrum for various defective formations (pure sample, anion vacancy and cationic interstitial) in SSS of  $\text{In}_x\text{Tl}_{1-x}\text{I}$  ( $x = 0.125, 0.25, 0.375, 0.5, 0.625$ ).

### 2. METHOD OF CALCULATIONS

In order to determine the band structure of  $\text{In}_x\text{Tl}_{1-x}\text{I}$  SSS we used the density functional theory (DFT) first principles method based on the nonlocal pseudopotentials. The calculation method used is described in details in Refs. [6, 7]. The main details of the method are following.

1. The total electron energy of the crystals was calculated self-consistently within the functional of the local density approximation (LDA).

2. The electron energy and density were determined using the Kohn-Sham equation [8].

3. For the ion potentials, the ultra-soft pseudopotentials of Vanderbilt [9] were used. For the exchange-and-correlation functional, the Coperley-Alder formula and the Gell-Mann-Bruckner expression in the high-density limit were used. The distribution of the charge

\* [Andriy.Kashuba@lnu.edu.ua](mailto:Andriy.Kashuba@lnu.edu.ua)

density was calculated by the method of special points with the use of the charge damping technique.

4. For each crystal structure, the relaxation of ion positions was performed on the basis of the calculated atomic forces and the integral stress of the unit cell. A convergence of the relaxation procedure was considered to be achieved when the values of the forces acting on the atoms were below the value of 0.05 eV/Å and the volumetric stress was less than 0.1 GPa. Calculations have been performed for the following indices  $x$  of the indium vs thallium content: 0.125, 0.25, 0.375, 0.5, 0.625.

### 3. RESULTS AND DISCUSSION

#### 3.1 Band Structure

The calculations were carried out along the main symmetrical directions of the Brillouin zone (BZ) (see Fig. 1). The band energy diagrams of the "ideal" structure of  $\text{In}_x\text{Tl}_{1-x}\text{I}$  SSS were presented in [1]. Fig. 2 shows the band energy structures of  $\text{In}_{0.5}\text{Tl}_{0.5}\text{I}$  with defective formations (see Fig. 3).

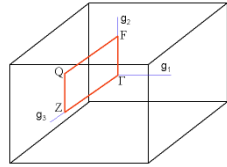


**Fig. 1** – Structure of Brillouin zone for  $\text{In}_x\text{Tl}_{1-x}\text{I}$  SSS:  $g_1$ ,  $g_2$ ,  $g_3$  – vectors of the reciprocal lattice

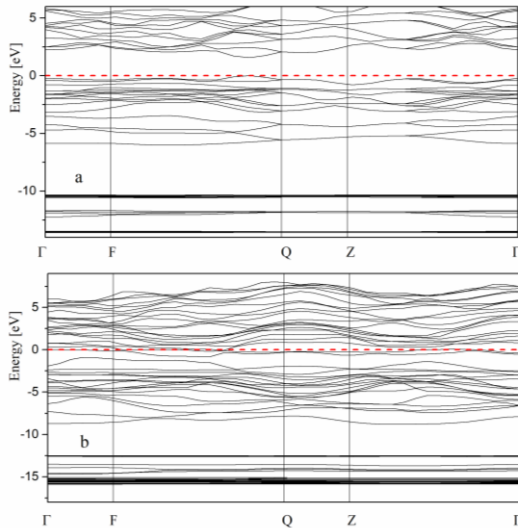


**Fig. 2** – Band energy diagrams of  $\text{In}_{0.5}\text{Tl}_{0.5}\text{I}$  crystal (a) and interstitial of Tl (b)

The introduction of a cation (anionic and cationic vacancies) in the interstitial cause's quasimetalization of the bonds what leads to a shift of the Fermi level into the conduction band. This feature can give rise to appearance of the quasimetallic bonds in  $\text{In}_x\text{Tl}_{1-x}\text{I}$  SSS. According to the experimental and theoretical results, the smallest energy intervals of the band gap are localized far from the  $\Gamma$  point. This is true for all compounds of the  $\text{A}^{\text{III}}\text{B}^{\text{VII}}$  class, both cubic and orthorhombic, and it follows, mainly, from the electronic

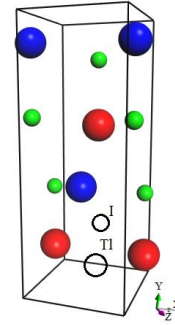


**Fig. 3** – Crystal lattice of  $\text{In}_{0.5}\text{Tl}_{0.5}\text{I}$  SSS with vacancy of I and interstitial of Tl (Tl-blue, In- green, I-red balls)

configuration of these "ten electrons" compounds with their excess  $s$ - electronic pair of a metal. When comparing the theoretical results with the experimental data, one must keep in mind the undervaluation of the band gap in the case of calculations in the approximation of local density. For agreeing and confirming the above assumptions a study of the conductivity of ideal samples and conduction spectra for the samples with defective formations in SSS  $\text{In}_x\text{Tl}_{1-x}\text{I}$  has been carried out.

#### 3.2 Effective Electron Mass

As it is known from the physics of solid state, the value of an effective electron mass ( $m^*$ ) indicates a reply of the electron in crystal on the external electric field and is usually presented in terms of the free electron mass  $m_e$ . The effective electron mass  $m^*$  may be both positive and negative, as well as the corresponding absolute value  $|m^*|$  may be both much larger and much smaller than the free electron mass  $m_e$ .

Information on the quantitative value of  $m^*$  for a material is important because this value determines the dynamics of electron conductivity in it and therefore is significant for the corresponding practical applications. One of the goals of the present study is to find out the relation between the indium vs. thallium content  $x$  in  $\text{In}_x\text{Tl}_{1-x}\text{I}$  SSS and the corresponding effective electron mass  $m^*$ .

The effective electron mass  $m^*$  is usually defined by the following relation from the band structure calculations [10],

$$\frac{1}{m^*} = \frac{4\pi^2}{h^2} \frac{d^2 E(k)}{dk^2} \quad (1)$$

where  $h$  is the Planck constant,  $E(k)$  is the dependence of the band energy  $E$  on the electron wave vector  $k$ . For the case of  $\text{In}_x\text{Tl}_{1-x}\text{I}$  SSS, the effective electron mass  $m^*$  was calculated at the minimum of the conduction band energy located between the high symmetry  $Z$  and  $\Gamma$  points of BZ. At this  $k$ - point, the smallest energy gap between the valence and conduction bands ( $E_g$ ) of  $\text{In}_x\text{Tl}_{1-x}\text{I}$  SSS also takes place. We have found that the higher the doping concentration of thallium ( $1-x$ ) in the non-defective  $\text{In}_x\text{Tl}_{1-x}\text{I}$  SSS, the larger the corresponding effective electron mass  $m^*$ .

$$\frac{m_{m=0.375}^*}{m_{m=0.875}^*} \approx 8.2$$

The choice of the  $k$ - point for the theoretical determination of the effective electron mass is caused by the fact that experimental determination of  $m^*$  using the edge luminescence is possible only from the minimum of conduction band as an initial energy state at this  $k$ -point. Similar experimental studies of the effective electron mass on the basis of other minima of the band energy dependences  $E(k)$  are not known.

### 3.3 Electron Mobility and Conductivity

According to the semiconductor theory [11-16] the specific conductivity  $\sigma$  of a material is dependent on the charged particles mobility ( $\mu$ ),

$$\sigma = nq\mu \quad (2)$$

Here  $q$  is the particle's charge and  $n$  is the charged particles concentration. That is why the dependence of the electron mobility  $\mu$  on the indium vs. thallium content  $x$  of  $\text{In}_x\text{Tl}_{1-x}\text{I}$  SSS is of interest also for the probable practical applications of the material. It is known also that for the case of the high doped semiconductors, the heating effects might be neglected in the conductivity process in comparison to the electron scattering by the ionized impurities, which becomes a dominating factor [10-16].

The electron mobility  $\mu$  is associated with an impurity of the  $i$ -type may be presented by the following relation [12],

$$\mu_i = \frac{q\tau_i}{m^*} \quad (3)$$

where  $\tau_i$  is the relaxation time, which is inversely proportional to the ionized impurity concentration  $n_i$ ,

$$\tau_i \propto n_i^{-1}T^{3/2} \quad (4)$$

Here  $T$  is the thermodynamic temperature. Then, for two different impurity concentrations of thallium,  $n_1$  and  $n_2$  ( $n_2 > n_1$ ), one can obtain the following relation,

$$\frac{\mu_2}{\mu_1} = \frac{\tau_2 q m_1^*}{\tau_1 q m_2^*} = \frac{n_1 m_1^*}{n_2 m_2^*} \approx 0.2 \quad (5)$$

The ratio  $\mu_2/\mu_1 \approx 0.2$  corresponds to the electron mobilities'  $\mu_2$  in  $\text{In}_{0.375}\text{Tl}_{0.625}\text{I}$  and  $\mu_1$  in  $\text{In}_{0.875}\text{Tl}_{0.125}\text{I}$  SSS.

According to the relation (2), the ratio of conductivities corresponding to two different doping concentrations  $n_2$  and  $n_1$  of thallium may be estimated as,

$$\frac{\sigma_2}{\sigma_1} = \frac{n_2 \mu_2}{n_1 \mu_1} = \frac{m_1^*}{m_2^*} \approx 8 \quad (6)$$

Here,  $\sigma_1$  is the specific electron conductivity for  $\text{In}_{0.875}\text{Tl}_{0.125}\text{I}$  and  $\sigma_2$  for  $\text{In}_{0.375}\text{Tl}_{0.625}\text{I}$  SSS.

One however should remember that the above estimations of the values  $\mu_2/\mu_1$  and  $\sigma_2/\sigma_1$  have been obtained at two simplifications: (1) the charge concentrations  $n_1$  and  $n_2$  for the impurity electrons (see Eq. 2) are identified as the corresponding impurity concentrations of thallium atoms; (2) the value of  $m_1^*/m_2^*$  corre-

sponds to the non-defective  $\text{In}_x\text{Tl}_{1-x}\text{I}$  SSS's, where the electric charges associated with interstitials of thallium atoms are absent. In the real case, two kinds of thallium atoms may exist in  $\text{In}_x\text{Tl}_{1-x}\text{I}$ : (1) thallium substituting indium in its crystal symmetry positions and (2) interstitial thallium. The above mentioned simplifications may cause the values  $\mu_2/\mu_1$  and  $\sigma_2/\sigma_1$  to be a bit larger but they can't change the final conclusion that the electron conductivity of  $\text{In}_x\text{Tl}_{1-x}\text{I}$  SSS is decreasing with increase of the doping concentration of thallium.

### 3.4 Optical Conductivity Spectra

Fig. 4 and 5 show the conductivity spectra of SSS  $\text{In}_{0.5}\text{Tl}_{0.5}\text{I}$  with defective formations. These spectra were determined from the band energy diagrams according to the following relationships:

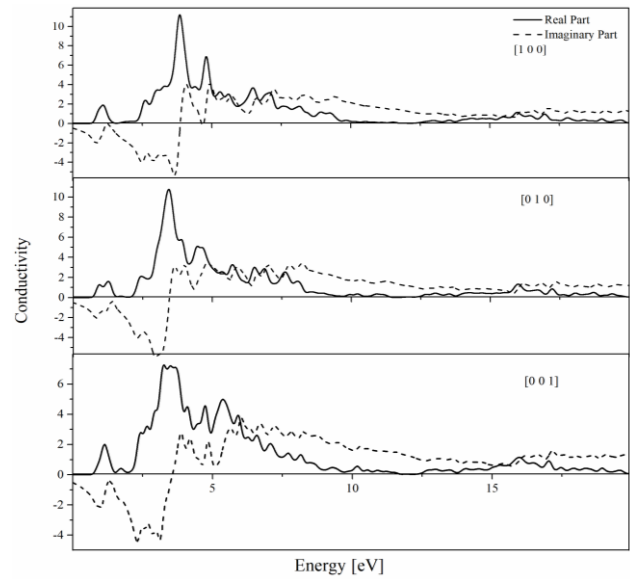


Fig. 4 – Conductivity spectra of  $\text{In}_{0.5}\text{Tl}_{0.5}\text{I}$  crystal with I vacancy in polarized light

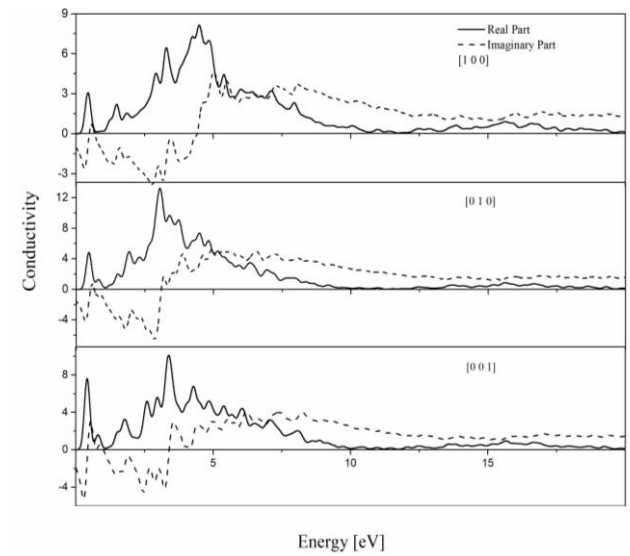


Fig. 5 – Conductivity spectra of  $\text{In}_{0.5}\text{Tl}_{0.5}\text{I}$  crystal with Tl interstitial in polarized light

$$\varepsilon = \varepsilon_1 + i \cdot \varepsilon_2 = (n + i \cdot k) \quad (7)$$

$$\sigma = \sigma_1 + i \cdot \sigma_2 = -i \cdot \frac{\omega}{4\pi} \cdot (\varepsilon - 1) \quad (8)$$

First-principles calculations of density state of electron and optical properties were publication in Ref. [4].

It is seen from Fig. 4 that anionic and cationic vacancies (anionic interstitials) do not significantly affect the behavior of conduction spectra and are typical for semiconductors [10-15]. At the same time introduction of the cation in the interstitial location leads to a displacement of the conduction spectrum (the real component), which is characteristic of metal samples (Fig. 5) [10, 11].

Figure 4 and 5 shows the conductivity spectra of SSS's  $\text{In}_x\text{Tl}_{1-x}\text{I}$  at normal pressure and exhibits the metallic nature of SSS's  $\text{In}_x\text{Tl}_{1-x}\text{I}$ , since the (photo-)

conductivity begins with zero photon energy. However, photoconductivity of SSS's  $\text{In}_x\text{Tl}_{1-x}\text{I}$  increases due to the result of absorbing photons.

## CONCLUSION

In this work, the band-energy spectrum of "ideal" and defective samples of  $\text{In}_x\text{Tl}_{1-x}\text{I}$  SSS has been investigated from the first principles. On the basis of the band-energy spectrum, effective electron mass, mobility, and conductivity have been calculated. It is established that the total conductivity decreases with increasing the thallium component. Using the experimental results the cause of occurrence of  $n$  conductivity in  $\text{In}_{0.5}\text{Tl}_{0.5}\text{I}$  SSS has been established when was recorded experimentally. The conductivity spectra of  $\text{In}_{0.5}\text{Tl}_{0.5}\text{I}$  for different defective formations have been investigated and shown that the cationic interstitials cause quasimetallization of the samples.

## REFERENCES

1. A.V. Franiv, V.Y. Stadnyk, A.I. Kashuba, R.S. Brezvin, O.V. Bovgira, A.V. Futei, *Opt. Spectroscopy*. **123**, 177 (2017).
2. A.I. Kashuba, A.V. Franiv, V.A. Franiv, *J. Nano-Electron. Phys.* **10** No 1, 01013 (2018).
3. Y.O. Dovhyi, A.V. Franiv, S.V. Ternavska, *Ukr. J. Phys. Opt.* **2**, 141 (2001).
4. A.I. Kashuba, M. Piasecki, O.V. Bovgyra, V.Yo. Stadnyk, P. Demchenko, A. Fedorchuk, A.V. Franiv, B. Andriyevsky, *Acta Physica Polonica A* **133**, 68 (2018).
5. G.A. Ilchuk, *J. Non-Crystal. Solid.* **352**, 4255 (2006).
6. R. Zallen, M.L. Slade, *Solid State Commun.* **17**, 1561 (1975).
7. M.I. Kolinko, R.Y. Bibikov, *J. Phys.: Condens. Matter.* **95**, 167 (1994).
8. M.I. Kolinko, O.V. Bovgyra, M. Piasecki, *Low Temp. Phys.* **27**, 153 (2001).
9. S.V. Syrotyuk, I.V. Semkiv, H.A. Ilchuk, V.M. Shved, *Condensed Matter Phys.* **19**, 43703 (2016).
10. W. Kohn, L.J. Sham, *Phys. Rev. A* **140**, A1133 (1965).
11. D. Vanderbilt, *Phys. Rev. B* **41**, 7892 (1990).
12. Zhao Yinnü, Yan Jinliang, Xu Chengyang, *J. Semiconductor.* **36**, 012003 (2015).
13. P.Y. Yu, M. Cardona, *Fundamentals of Semiconductors: Physics and Materials Properties*, 205 (Springer: 2010).
14. Qingyu Hou, Wencai Li, Zhenchao Xu, Chunwang Zhao, *Int. J. Modern Phys. B* **30**, 1650001 (2016).
15. Qingyu Hou, Ji Jun Li, C.W. Zhao, Chun Ying, Yue Zhang, *Physica B* **406**, 1956 (2011).
16. Qi-Jun Liu, Zheng-Tang Liu, Li-Ping Feng, Hao Tian, *International Scholarly Research Network ISRN Condensed Matter Physics*, 290741 (2011).
17. M.Z. Hasan, M.M. Hossain, M.S. Islam, F. Parvin, A.K.M.A. Islam, *Computat. Mater. Sci.* **63**, 256 (2012).
18. Jian Sun, Hui-Tian Wang, *Phys. Rev. B.* **71**, 125132 (2005).